Electrohydrodynamic Mixing in Microchannels

C. Tsouris, C. T. Culbertson, D. W. DePaoli, S. C. Jacobson, V. F. de Almeida, and J. M. Ramsey
Oak Ridge National Laboratory, Oak Ridge, TN 37831

Electrohydrodynamic flow generated by the motion of charge carriers in an electric field was investigated for rapid mixing in microchannel devices. A "tee" geometry of channels ranging from 40 to 110 μm in width and 30 to 60 μm in depth was used to contact two miscible fluids, such as alcohols. A fluorescent dye (Rhodamine B) was used to quantify mixing. A potential difference ranging from 0 to 900 V was applied between two electrodes separated by a distance of 450 μm, resulting in field strengths ranging from 0 to 2×10^6 V/m. Results show that when no electric field is applied, mixing of the two streams is driven by diffusion and is, therefore, slow. The mixing length, at which the concentration across the channel becomes essentially uniform, decrease significantly as the applied voltage was increased. There seems to be a threshold of applied voltage below which mixing is not enhanced by the electric field under the conditions studied. In strong electric fields, the mixing length was less than 150 μm, while in the absence of an electric field, the mixing length was greater than 5,000 μm.

Introduction

A variety of elementary microchips capable of performing simple chemical analyses have been demonstrated in the past decade using both hydraulic and electrokinetic fluid control. Electrokinetically driven processes, however, have been given more attention and have been demonstrated for mixing and reacting reagents, injection or dispensing of samples, chemical separations, flow injection analysis, and cytometry (Bousse et al., 2000; Dolnik et al., 2000; Jacobson and Ramsey, 1997, 1998; Jakeway et al., 2000). These miniature devices have shown performance either equivalent to or better than that of conventional laboratory devices. Other significant advantages of microchip-based chemical separations are the small volumes that can be analyzed, the ability to monolithically integrate sample processing and analysis, and the low cost of replication. Early efforts demonstrating the integration of sample processing include postseparation (Jacobson et al., 1994a; Fluri et al., 1996) and preseparation (Jacobson et al., 1994b) derivitization of amino acids coupled to electrophoretic separations. On-chip DNA restriction digestions (Jacobson and Ramsey, 1996) and polymerase chain reaction (PCR) amplifications (Waters et al., 1998a,b; Woolley et al., 1996) have been coupled with electrophoretic fragment sizing on integrated microchips. In addition, competitive immunoassay experiments have been performed on a microchip device that included fluidic elements for mixing of the sample with reagents, incubation, and electrophoretic separations (Chiem and Harrison, 1998). The ability to manipulate reagents and reaction products "on-chip" suggests the eventual ability to perform virtually any type of "wet-chemical" process on a microfabricated device consisting of several microchannels. By implementing multiple processes in a single device (vertical integration), these small fluid quantities can be manipulated from process to process efficiently and automatically under computer control. The serial integration of multiple analysis steps can be combined with parallel expansion of processing capacity by replicating microfabricated structures (such as parallel separation channels) on the same device.

Fluid mixing in microchannels

The ability to carry out complex operations on integrated microfluidic devices depends in large part upon the ability to mix fluidic streams in microchannels. The mixing ratio for the fluids in such operations will be dictated by both the forces applied to the termini of the channels and the geometry of the channels. For example, two fluid streams can be proportionately mixed in any ratio from 0 to 100% for either stream at a "tee" intersection simply by varying the relative electric-field strengths in the two input channels (Harrison et al., 1993). In addition, by properly designing the microchannel manifold, one can accomplish parallel and serial electrokinetic mixing using a simple voltage-control circuit (Jacobson et al., 1999). This minimizes the high-voltage hardware required to operate the microfluidic chip. Mixing on microflu-

Correspondence concerning this article should be addressed to C. Tsouris.
Current address of C. T. Culbertson, Dept. of Chemistry, Kansas State University, Manhattan, KS 66506.

idic devices typically occurs by the interplay of molecular diffusion and pressure-driven convection (that is, dispersion) in the laminar regime. This process may not be sufficiently fast for some analyses. Mixing rates can be enhanced by using the principle of flow lamination (Bessoth et al., 1999), whereby the streams are divided into n laminae with widths $1/n$ of the original channel. This results in faster mixing by a factor of n^2.

More recently, in order to enhance mixing in microchannels, Liu et al. (2000), Stroock et al. (2002), and Johnson et al. (2002) introduced passive mixing using specially designed channels with various microstructures. Oddy et al. (2002), on the other hand, introduced active mixing by means of electrokinetic instability caused by a sinusoidally oscillating electrokinetic flow. Choi and Ahn (2000) introduced an active micromixer using electrohydrodynamic convection.

Another approach to efficiently mix fluidic streams in microchannels is demonstrated here. This method is based on electrohydrodynamic (EHD) flows generated by the motion of charge carriers in an electric field (Gross and Porter, 1966; Felici, 1972a,b; Crowley et al., 1985). It recently has been shown that EHD flows may cause pumping, spraying, and mixing of mildly conductive fluids including water and alcohols (Tsouris et al., 1998, 2000). EHD flow is a basic mechanism of electrical conduction in fluids involving mechanical transport of space charge by the induced streaming motion. Electrostatic forces are the main cause of this motion, whereas polarization forces (dielectrophoretic) play a minor role, if any, unless alternating currents are applied. In the case of applied direct currents, the effect of polarization forces is limited to regions of intense electric-field gradients, typically near an electrode surface; however, no sustained fluid motion will arise. Since the existence of space charge is a condition for the development of EHD flows, highly conductive liquids, wherein bulk electroneutrality holds, are not susceptible to this motion. As is well known from the theory of electrolytes, the motion arising in conductive systems results from excess mobile charge within the electrical double layer. When this layer is small compared to the system size, the driving force for fluid motion is also small. By contrast, when space charges are present, strong fluid motion is feasible due to the pull of surrounding fluid by means of molecular drag, and the resulting motion is known as EHD flow. In general, space charges either exist in the fluid or are created either in bulk or at an electrode. Charges created at the surface of an electrode are typically a result of electron-transfer reactions (polar fluids) or field-emission/field-ionization (nonpolar fluids), so-called charge injection. Charges created in bulk may be the result of dissociation in the presence of a strong electric field. The interaction of the space charges subjected to the applied electric field and the surrounding fluid is often very complex and coupled.

EHD phenomena have been long noted by scientists (Faraday, 1838); however, it was not until the early twentieth century that the hypothesis was made that fluid motion between parallel plates resulting from the presence of space charges could greatly affect electrical conduction (Tobazeon, 1984). The mathematical formulation of EHD involving the coupling of Coulomb force to the Navier-Stokes equations also appeared several decades ago (for example, Melcher, 1981; Tobazeon, 1984). Despite numerous studies in the past decades on electrical conduction in fluids—in particular, for good dielectrics (Tobazeon, 1995)—much remains to be done so the subject can guide new technological applications. EHD mixing, for instance, could be suitable for such fluids as leaky dielectrics with electrical conductivities of at least 2 to 3 orders of magnitude lower than that of aqueous solutions of relatively low electrolyte concentration. Such fluids are alcohols and other organic solvents, which can be used for chemical analysis, as well as chemical synthesis in microfabricated reactor chips (Salimi-Moosavi, 1997; Haswell, 2001).

This research addresses for the first time the process of mixing in microfluidic devices by means of EHD flows. EHD mixing of alcohols at a tee intersection is experimentally investigated using polymer-based microchannels.

Experimental Methods

Chemicals

The chemicals used here, Rhodamine B (RhB) and 1-butanol, were obtained from Eastman Chemical Co. (Kingsport, TN) and EM Science (Gibbstown, NJ), respectively. Rhodamine B chloride ($C_{28}H_{31}O_3N_2Cl$) was dissolved in 1-butanol in this experiment. The spectrum of this laser dye is known to depend on temperature, solvent, and concentration (Hinckley et al., 1986). At low enough concentration (typically 10^{-5} M) in protic solvents, the dye exists as an equilibrium mixture of a colorless lactone and a colored zwitterion. The position of the equilibrium depends on both solvent hydrogen-bond donating ability and solvent dielectric/polarization characteristics. At a higher temperature, the equilibrium shifts toward the less polar lactone. At higher concentration, two other forms of the dye appear, namely, the cation and the dimer; both forms are highly colored, too, and their presence can interfere with the light intensity measured. In equilibrium at 25°C, the percentage of the zwitterion form in 1-butanol is 54%, the maximum light absorbance (approximately 0.5) occurs at a the wavelength of 540 nm, and a small absorbance occurs at wavelengths greater than 580 nm or less than 440 nm (the fluorescence-emission wavelength maximum is 585 nm). No careful control of the Rhodamine B solution was made except to use concentrated solutions in equilibrium, therefore, the pointwise light intensity measured in the microchannel may reflect the existence of more than one compound. In addition, the presence of an externally imposed intense electric field by means of direct contact of a metal electrode with the solution may have disturbed the equilibrium, in particular, at points near the electrode surface where electron-transfer reactions take place. Nevertheless, the illumination setup was able to capture fluorescence light at wavelengths greater than 575 nm.

Microchip design

The masks for photolithographically patterning the chips and integrated electrodes were designed in-house with MiniCAD (Diehl Graphsoft, Inc., Columbia, MD) and fabricated by HTA Photomask (San Jose, CA). Negative channel masters were created in Nano XP SU-8 5 (Microchem Corp., Newton, MA). The SU-8 was spin coated onto a clean glass microscope slide at 11.4 rps for 20 s; baked for 180 s at 65°C, followed by a 2-h bake at 95°C; and afterwards slowly cooled.

The SU-8 film was then placed in direct contact with the mask and exposed to ultraviolet light. After exposure, the SU-8 was baked at 90°C for 300 s, slowly cooled, agitated in SU-8 developer (Microchem) for 300 s, rinsed with fresh developer, and air dried. The ridges on the resultant negative mold were measured using a stylus-based surface profiler (P-10, Mountain View, CA).

For the electrode patterning, glass cover plates were prepared by ultrasonically treating the plates in a detergent-based cleaning solution (GP Cleaning Solution, Branson, Danbury, CT), rinsing in deionized water, rinsing in methanol, and then drying with argon. After cleaning, 50 nm of titanium was sputtered onto the entire surface at 200°C, followed by sputtering with 100 nm of gold. The metallized cover plate was then spin coated with photoresist (Microposit 1813, Shipley, Marlborough, MA), masked with the desired electrode pattern, and exposed to ultraviolet light. Exposed photoresist was subsequently developed (Microposit MF-319, Shipley) and removed, leaving a protective layer of photoresist covering the electrode-patterned regions. Sequentially, gold (0.6 M KI, 0.1 M I_2 in H_2O) and titanium etchants (Type TFTN, Transene Co., Danvers, MA) were used to remove unwanted metallization, leaving the desired electrode pattern.

To create the channel manifold, polydimethylsiloxane (PDMS) (Sylgard 184, Dow Corning, Midland, MI) was poured over the negative SU-8 molds and cured at 65°C for 2 h. The PDMS structures were removed from the mold and reversibly sealed to a glass slide onto which the electrode pattern was fabricated to form a closed-channel network. A 2-mm-diameter metal tube, sharpened on one end, was used to create (that is, by punching) the reservoirs at the end of the three channels. A chip with electrodes is presented in Figure 1. Channels 1, 2, and 3 were 5.7, 5.5, and 12.7 mm long, respectively. All of the channels were 37 μm deep, 106 μm wide at the bottom, and 50 μm wide at the top. The distance between the active electrodes was 450 μm.

Experimental apparatus

All experiments were performed with the microchip on the stage of a Nikon-TE300 inverted microscope equipped with an epi-illumination setup (Nikon, Melville, NY) and charge-coupled device (CCD) camera (TEA/CCD-770-EM1, Princeton Instruments, Trenton, NJ). A BV1 filter cube was used to select the appropriate excitation, dichroic, and emission wavelengths for RhB detection (see Figure 2). For image acquisition, the CCD camera was operated using IPLab (Scanalytics, Inc., Fairfax, VA), and all of the data were processed using IGOR Pro (Wavemetrics, Inc., Lake Oswego, OR).

Liquids were moved through the chip by applying vacuum aspiration to reservoir C at the end of channel 3. The absolute pressure was determined by using an in-line pressure gauge (SC Series Pressure Transducer 060-6833-02, Sensotec, Columbus, OH) and adjusted via an in-line valve. The potentials applied to the intrachannel electrodes were generated using two independent and remotely programmable high-voltage (0- to 10-kV) power sources from a multiple-source supply (model 2866, Bertan, Hicksville, NY) and controlled with in-house code written using LabVIEW graphical instrumentation software (National Instruments, Inc., Austin, TX).

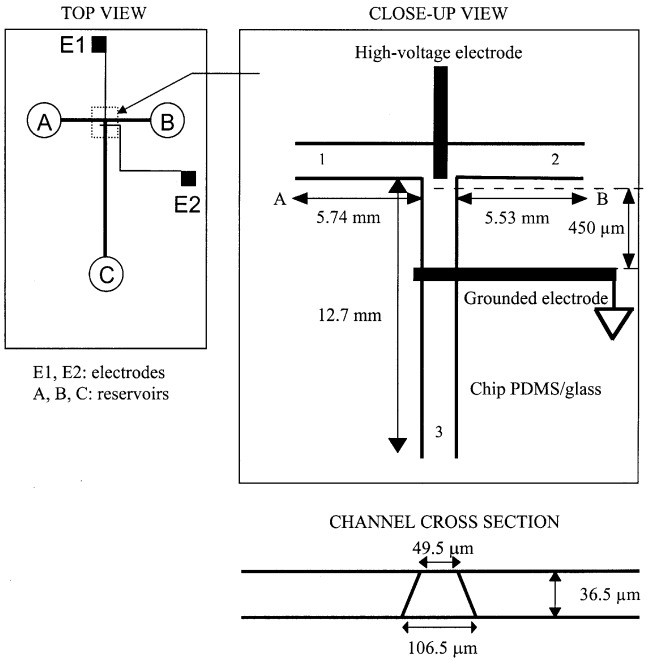

Figure 1. Chip used for the experiments.

In the experiments discussed here, electrode E1 in Figure 1 was negatively charged and electrode E2 was grounded.

Results and Discussion

Figure 3 shows the microchip manifold used in the experiments reported below with all of the channels filled with RhB-doped butanol. To study EHD-induced mixing performed on this chip, we flowed RhB-doped butanol from reservoir A through channel 1 and neat butanol from reservoir B through channel 2 (see Figures 1 and 4). The effects of both flow rate and applied voltage were examined. Three levels of vacuum were imposed over reservoir C at 0.924×10^5, 0.848×10^5, and 0.676×10^5 Pa, while keeping the ambient pressure at 0.972×10^5 Pa over reservoirs A and B. The corresponding flow rate was estimated from the Poiseuille formula (White, 1991) applied to the three sections of the microchannel, assuming an equivalent rectangular cross section

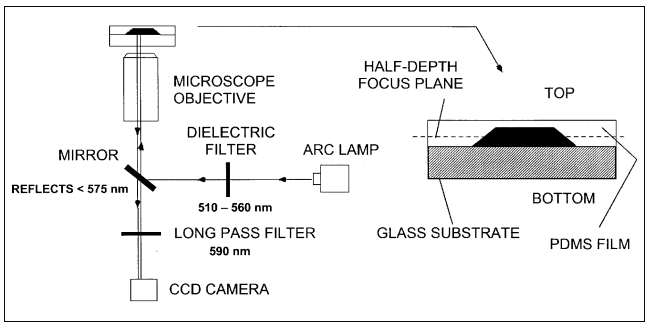

Figure 2. Experimental setup for flow visualization in microchannels.

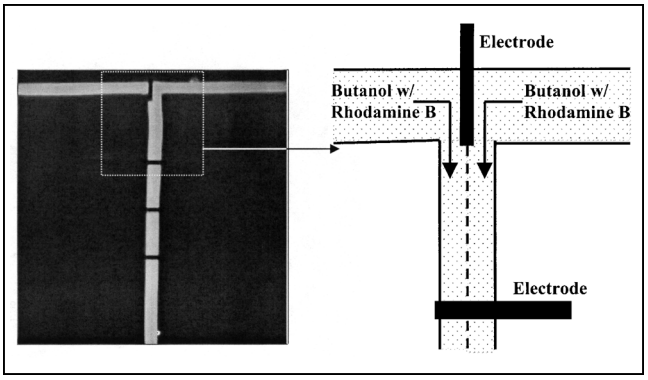

Figure 3. Microchip with all channels filled with Rhodamine B.

(36.5 μm for the depth and 78 μm for the width) with the same hydraulic radius as the measure of the cross section. Using the dynamic viscosity value of $2.54\ 10^{-3}$ kg/m·s for the fluid, the three corresponding estimated flow rates were 27, 70, and 167 nL/s (with combined average speeds of 9.6, 24.5, and 58.7 mm/s, respectively, after the tee intersection). Tables 1 and 2 list geometric quantities, physical properties, and flow parameters calculated from measured pressure drop.

The voltage required to generate EHD mixing was applied between the electrode that terminated at the tee intersection and the center electrode traversing the center channel. The distance between these electrodes was 450 μm, and the direct-current voltage was varied from 0 to 900 V, resulting in field strengths ranging from 0 to 2×10^6 V/m. With no applied voltage, mixing was diffusion limited at all velocities tested. This process was rather slow, and on the time and distance scale of the experiments, essentially no mixing was observed. Figure 4 shows the results obtained with the midrange flow rate tested, 70 nL/s (24.5 mm/s). By applying an appropriate range of voltages between the electrodes, mixing could be completed almost instantly once the threshold for EHD flow was surpassed. The onset of EHD flow occurred at 450 V $\pm$50 V over the course of an experiment as well as from experiment to experiment. At voltages below 400 V (0.89×10^6 V/m), EHD mixing was never observed at any of the flow rates. However, at 600 V (1.33×10^6 V/m), visually detectable EHD flow was always generated at all of the flow rates tested.

Shown in Figure 4 (bottom) are also two graphs, where the cross sections of normalized intensity is plotted vs. channel width for 400 and 900 V at a number of points from 50 to 460 μm downstream from the intersection. It is clear from these

Table 1. Geometrical Quantities for Channel of Equivalent Rectangular Cross Section and Physical Properties

	Quantities	
d = channel depth	36.5	μm
W = channel width	78	μm
ℓ_L = length of channel left arm	5.74	mm
ℓ_R = length of channel right arm	5.53	mm
ℓ_B = length of leg	12.7	mm
μ = fluid viscosity	2.54×10^{-3}	kg/m s
ρ = fluid mass density	8.06×10^2	kg/m^3
$\mathfrak{D}$ = diffusion coefficient	1.7×10^{-10}	m^2/s

Table 2. Flow Parameters for Three Values of Mass Flow Rate

Parameter	27 nL/s	70 nL/s	167 nL/s
Mean flow speed (ω), mm/s	9.6	24.5	58.7
Reynolds number $Re = \frac{2\rho\omega}{\mu}\frac{dW}{d+W}$	0.2	0.4	0.9

figures that no mixing occurs at 400 V, while at 900 V, good mixing is noticeable even at the shortest distance, 50 μm downstream from the intersection.

To better quantify the mixing, the spatial distribution of RhB was determined from fluorescence intensity measurements. The intensity distributions for five images collected by the CCD camera were averaged and flat-field corrected for differences in intensity. The intensity was normalized to the intensity of the RhB-doped inlet stream (C_x), approximately

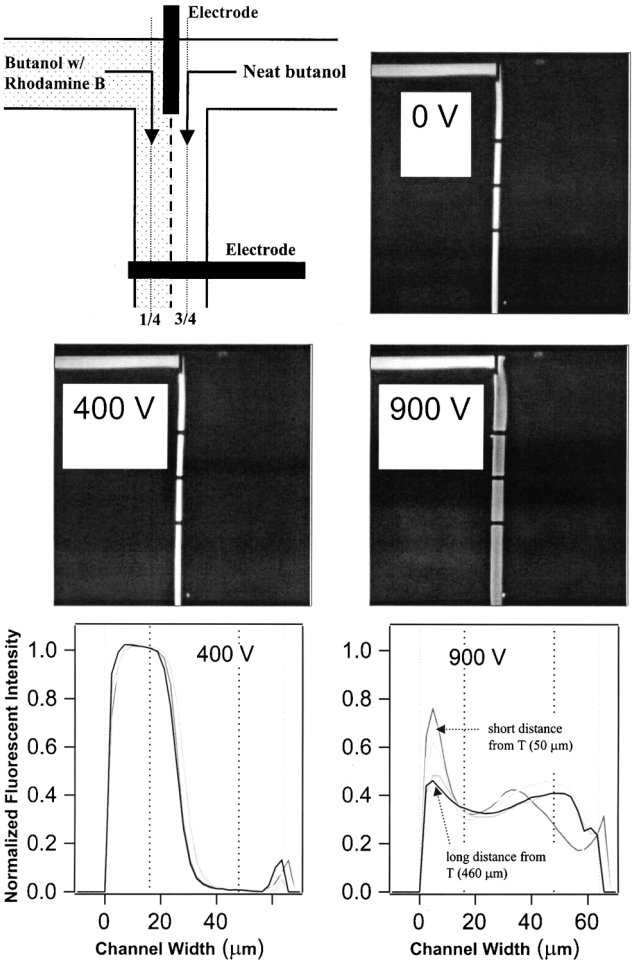

Figure 4. Microchip with Rhodamine B in butanol in the left channel and neat butanol in the right channel at varying values of applied voltage.

The flow rate in the vertical channel is 70 nL/s (24.5 mm/s). At 0 and 400 V, mixing is diffusion limited; therefore, it is ineffective, as demonstrated by strong fluorescence in the left half of the downstream (vertical) channel of the tee intersection. At 900 V, the dye is visible in the entire channel leaving the intersection and is less concentrated (as indicated by its intensity). The two graphs at the bottom show cross sections of dye concentration at 400 and 900 V at various positions downstream from the intersection.

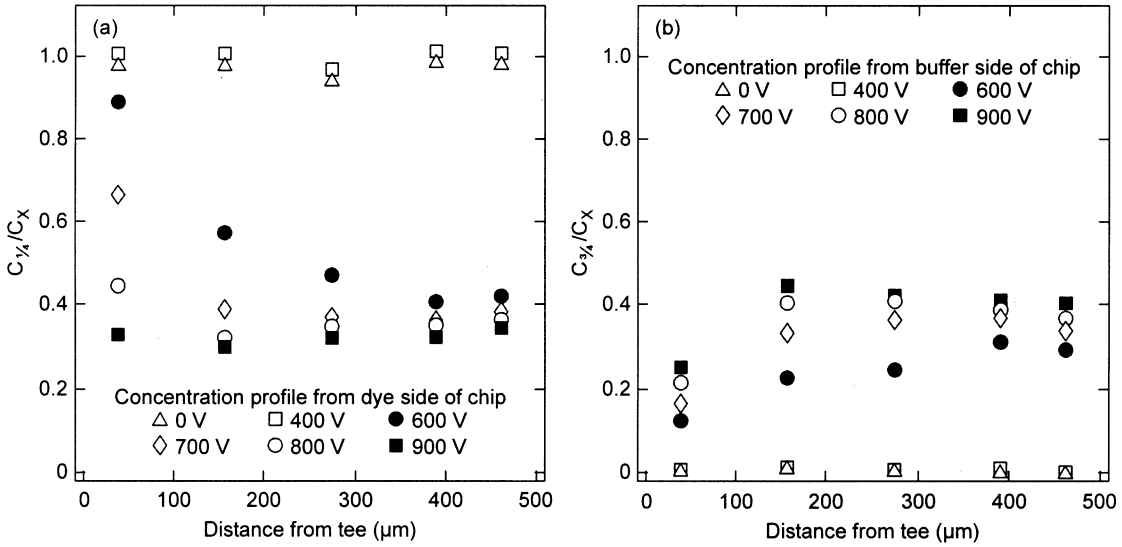

Figure 5. Concentration profiles of Rhodamine B in butanol downstream from the tee intersection at varying values of applied voltage.

(a) Ratio of concentration at 1/4 of the channel width to that at the channel left arm (see Figure 4); (b) ratio of concentration at 3/4 of the channel width to that at the channel left arm. Average flow speed: 24.5 mm/s.

50 μm upstream from the tee (left arm of the channel in Figure 4). Figure 5 shows representative cross sections of dye concentration taken from images of the flow at 70 nL/s, with both varying voltage and position downstream from the tee. The channel width in the profile plots corresponded to the channel width measured at half-depth using the surface profiler. No appreciable mixing occurred across the channel width at either 0 or 400 V (0.89×10^6 V/m), whereas at 800 or 900 V (1.78×10^6 or 2×10^6 V/m), mixing was substantial even at distances less than 150 μm downstream from the intersection, corresponding to 6 ms of mixing time. At intermediate voltages (600 or 700 V) enhanced mixing required a distance of 300 to 400 μm (12 to 16 ms).

Figure 6 shows the extent of mixing at each level of applied voltage for the case of 9.6 mm/s average flow speed. Values of mixing are reported as the normalized ratio of RhB concentrations at positions 1/4 and 3/4 of the channel width from the side of the channel where RhB was introduced vs. the applied voltage; ideally, a value of 1 would indicate essentially complete mixing. Because of differences in the flow resistance in the upper arms of the tee, the fluid contribution from these arms to the mixing channel was slightly unequal. The concentration ratios, therefore, were slightly below 1, which is the value that would be expected if the fluids were completely mixed and the contribution from the two channels was equal. However, a plateau in the extent of mixing was observed in most cases, as would be expected for complete mixing. The distance at which the plateau was reached varied with both velocity and applied voltage.

Summary

In summary, EHD flows have been shown to significantly improve fluid mixing over that encountered in conventional microsystems; this can be directly translated into smaller microdevice size. In microchannels where flow is driven either by pressure difference or electrokinetic transport (primarily electroosmosis), mixing is diffusion limited and is, thus, very slow. EHD flows can be superimposed to vigorously mix two streams at an intersection. The result is that EHD mixing can improve efficiency and selectivity of fast chemical reactions, improving speed and sensitivity within a much shorter channel length, allowing microchips of smaller dimensions to be used. In addition, EHD pumping and mixing can extend applicability of microsystems to organic fluids and to multiphase fluid systems.

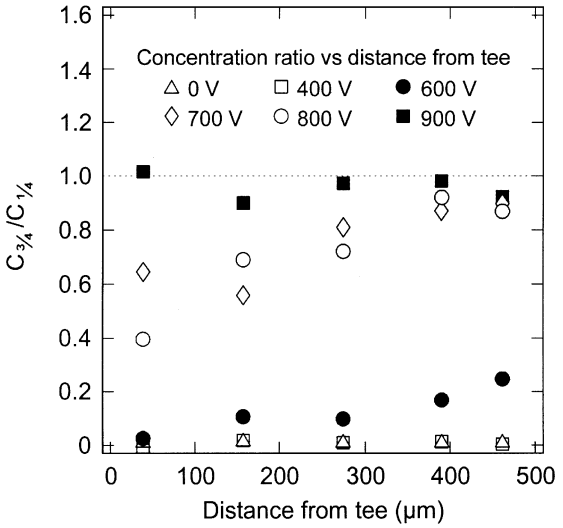

Figure 6. Concentration profiles of Rhodamine B in butanol downstream from the tee intersection at varying values of applied voltage; ratio of concentration at 3/4 of the channel width to that at 1/4 of the channel width.

See diagram in Figure 4. Average flow speed: 9.6 mm/s.

In general, EHD flows provide another tool to control fluid operations in microdevices. However, before they can be used in such applications, several issues must be resolved, including determination of the range of fluid and solid-state properties to which strong electric fields can be applied. In this study, we also investigated EHD mixing in aqueous solutions and found that because of the higher conductivity of the solution as compared with that of alcohols and other organic solvents, undesirable phenomena, including bubble generation and electrode corrosion, occur at the electrodes. Although EHD flows may be generated in organic fluids in which electrokinetic transport is limited, the physical properties of the system at which undesirable phenomena occur must be identified. In addition, the effect of electrode geometry and type of electric field (such as direct current, alternating current, and pulsed direct current) should be further investigated in future studies.

Additional theoretical work is needed to understand electrochemical mixing. Also, future studies should focus on the mathematical description of the onset of EHD flows in microchannels and investigate potential techniques to control such flows.

Acknowledgments

Research sponsored by the Laboratory Directed Research and Development Program of Oak Ridge National Laboratory (ORNL), managed by UT-Battelle, LLC for the U. S. Department of Energy under Contract No. DE-AC05-00OR22725, and by the Division of Chemical Sciences, Office of Basic Energy Sciences, U.S. Department of Energy. The authors are thankful to Dr. Marsha Savage for editing the manuscript.

Literature Cited

Bessoth, F. G., A. J. deMello, and A. Manz, "Microstructure for Efficient Continuous Flow Mixing," *Anal. Commun.*, **36**, 213 (1999).

Bousse, L., C. Cohen, T. Nikiforov, A. Chow, A. R. Kopf-Sill, R. Dubrow, and J. W. Parce, "Electrokinetically Controlled Microfluidic Analysis Systems," *Annu. Rev. Biophys. Biomolec. Struct.*, **29**, 155 (2000).

Chiem, N. H., and D. J. Harrison, "Microchip Systems for Immunoassay: An Integrated Immunoreactor with Electrophoretic Separation for Serum Theophylline Determination," *Clin. Chem.*, **44**, 591 (1998).

Choi, J.-W., and C. H. Ahn, "An Active Micro Mixer Using Electrohydrodynamic (EHD) Convection," Solid-State Sensor and Actuator Workshop, Hilton Head Island, SC, p. 52 (2000).

Crowley, J. M., P. Chang, D. Riley, and J. C. Chato, "EHD Induction Pumping in Annuli," *IEEE Trans. Elec. Insul.*, **EI-20**, 413 (1985).

Dolnik, V., S. Liu, and S. Jovanovich, "Capillary Electrophoresis on Microchip," *Electrophoresis*, **21**, 41 (2000).

Faraday, M., *Experimental Researches*, Vol. 1, Dover, New York, p. 507 (1838).

Felici, N., "D.C. Conduction in Liquid Dielectrics (Part I): A Survey of Recent Progress," *Direct Current*, **2**(3) (1972a).

Felici, N., "D.C. Conduction in Liquid Dielectrics (Part II): Electrohydrodynamic Phenomena," *Direct Current*, **2**(4) (1972b).

Fluri, K., G. Fitzpatrick, N. Chiem, and D. J. Harrison, "Integrated Capillary Electrophoresis Devices with an Efficient Postcolumn Reactor in Planar Quartz and Glass Chips," *Anal. Chem.*, **68**, 4285 (1996).

Gross, M. J., and J. E. Porter, "Electrically Induced Convection in Dielectric Liquids," *Nature*, **212**, 1343 (1966).

Harrison, D. J., K. Fluri, K. Seiler, Z. Fan, C. S. Effenhauser, and A. Manz, "Micromachining a Miniaturized Capillary Electrophoresis-Based Chemical-Analysis System on a Chip," *Science*, **261**, 895 (1993).

Haswell, S. J., "Miniaturisation—What's in it for Chemistry," *Micro Total Analysis Systems*, J. M. Ramsey and A. van den Berg, eds., p. 637 (2001).

Hinckley, D. A., P. G. Seybold, and D. P. Borris, *Spectrochimica Acta*, **42A**, 747 (1986).

Jacobson, S. C., and J. M. Ramsey, "Integrated Microdevice for DNA Restriction Fragment Analysis," *Anal. Chem.*, **68**, 720 (1996).

Jacobson, S. C., and J. M. Ramsey, "Microfabricated Devices for Performing Capillary Electrophoresis," *Handbook of Capillary Electrophoresis*, 2nd ed., Chap. 29, J. P. Landers, ed., CRC Press, New York, p. 827 (1997).

Jacobson, S. C., and J. M. Ramsey, "Microfabricated Chemical Separation Devices," *High-Performance Capillary Electrophoresis*, Vol. 146, Chap. 18, M. G. Khaledi, ed., Wiley, New York, p. 613 (1998).

Jacobson, S. C., L. B. Koutny, R. Hergenröder, A. W. Moore, Jr., and J. M. Ramsey, "Microchip Capillary Electrophoresis with an Integrated Postcolumn Reactor," *Anal. Chem.*, **66**, 3472 (1994a).

Jacobson, S. C., R. Hergenröder, A. W. Moore, Jr., and J. M. Ramsey, "Precolumn Reactions with Electrophoretic Analysis Integrated on a Microchip," *Anal. Chem.*, **66**, 4127 (1994b).

Jacobson, S. C., T. E. McKnight, and J. M. Ramsey, "Microfluidic Devices for Electrokinetically Driven Parallel and Serial Mixing," *Anal. Chem.*, **71**, 4455 (1999).

Jakeway, S. J., A. J. de Mello, and E. L. Russell, "Miniaturized Total Analysis Systems for Biological Analysis," *Fresenius' J. Anal. Chem.*, **366**, 525 (2000).

Johnson, T. J., D. Ross, and L. E. Locascio, "Rapid Microfluidic Mixing," *Anal. Chem.*, **74**, 45 (2002).

Liu, R. H., M. A. Stremler, K. V. Sharp, M. G. Olsen, J. G. Santiago, R. J. Adrian, H. Aref, and D. J. Beebe, "Passive Mixing in a Three-Dimensional Serpentine Microchannel," *J. MEMS*, **9**, 190 (2000).

Melcher, J. R., *Continuum Electromechanics*, The MIT Press, Cambridge, MA (1981).

Oddy, M. H., J. G. Santiago, and J. C. Mikkelsen, "Electrokinetic Instability Micromixing," *Anal. Chem.*, (2002).

Salimi-Moosavi, H., T. Tang, and D. J. Harrison, "Electroosmotic Pumping of Organic Solvents and Reagents in Microfabricated Reactor Chips," *J. Amer. Chem. Soc.*, **119**, 8716 (1997).

Stroock, A. D., S. K. W. Dertinger, A. Ajdari, I. Mezic, H. A. Stone, G. M. Whitesides, "Chaotic Mixer for Microchannels," *Science*, **295**, 647 (2002).

Tobazeon, R., "Electrohydrodynamic Instabilities and Electroconvection in the Transient and A.C. Regime of Unipolar Injection in Insulating Liquids: A Review," *J. Electrostatics*, **15**, 359 (1984).

Tobazeon, R., "Electrical Phenomena of Dielectric Materials," *Handbook of Electrostatic Processes*, Chap. 4, J.-S. Chang, A. J. Kelly, J. M. Crowley, eds., p. 51 (1995).

Tsouris, C., W.-T. Shin, and S. Z. Yiacoumi, "Pumping, Spraying, and Mixing of Fluids by Electric Fields," *Can. J. Chem. Eng.*, **76**, 589 (1998).

Tsouris, C., W.-T. Shin, S. Z. Yiacoumi, and D. W. DePaoli, "Electrohydrodynamic Velocity and Pumping Measurements in Water and Alcohols," *J. Colloid Interface Sci.*, **229**, 335 (2000).

Waters, L. C., S. C. Jacobson, N. Kroutchinina, J. Khandurina, R. S. Foote, and J. M. Ramsey, "Multiple Sample PCR Amplification and Electrophoretic Analysis on a Microchip," *Anal. Chem.*, **70**, 5172 (1998a).

Waters, L. C., S. C. Jacobson, N. Kroutchinina, J. Khandurina, R. S. Foote, and J. M. Ramsey, "Microchip Device for Cell Lysis, Multiplex PCR Amplification, and Electrophoretic Sizing," *Anal. Chem.*, **70**, 158 (1998b).

White, F. M., *Viscous Fluid Flow*, McGraw Hill, New York, (1991).

Woolley, A. T., D. Hadley, P. Landre, A. J. deMello, R. A. Mathies, and M. A. Northrup, "Functional Integration of PCR Amplification and Capillary Electrophoresis in a Microfabricated DNA Analysis Device," *Anal. Chem.*, **68**, 4081 (1996).

Manuscript received Apr. 26, 2002, revision received Dec. 17, 2002, and final revision received Apr. 21, 2003.